IIETA International Information and Engineering Technology Association
Advancing the World of Information and Engineering

Annales de Chimie - Science des Matériaux
Vol. 48, No. 2, April, 2024, pp. 291-301
Journal homepage: http://iieta.org/journals/acsm

Simulation-Based Evaluation of Alumina and Weldox Steel Panels Against National Institute of Justice Type IV Ballistic Threats

Fattah Maulana[1], Ubaidillah[1,2*], Adhe Lingga Dewi[3], Bhre Wangsa Lenggana[4], Sigit Puji Santosa[5], Yahya Ahmed Ali Alashwal[2]

[1] Department of Mechanical Engineering, Faculty of Engineering, Universitas Sebelas Maret, Surakarta 57126, Indonesia
[2] Department of Mechanical Engineering, Islamic University of Madinah, Madinah 42351, Saudi Arabia
[3] Computer Science Department, School of Computer Science, Universitas Bina Nusantara, Semarang 50144, Indonesia
[4] Industrial Engineering, Faculty of Engineering, Universitas Jenderal Soedirman, Purwokerto 53122, Indonesia
[5] Research and Development Department Head, Bandung 40285, Indonesia

Corresponding Author Email: ubaidillah_ft@staff.uns.ac.id

https://doi.org/10.18280/acsm.480215

Received: 16 October 2023
Revised: 22 March 2024
Accepted: 8 April 2024
Available online: 30 April 2024

Keywords:
ballistic performance, impact resistance, alumina and weldox 460 E steel, NIJ type IV standard, panel configurations, finite element simulation, ballistic testing simulation

ABSTRACT

This study sought to evaluate several panel configurations consisting of Alumina and Weldox 460 E Steel with the objective of advancing our comprehension of ballistic performance and impact resistance. The crucial parameters of Velocity Ballistic Limit (Vbl), depth of penetration (DOP), Deflection, and the deformation of projectiles and panels were thoroughly and rigorously investigated. The present study expands upon the existing body of research, drawing upon the groundwork established by previous studies. The validation is achieved by conducting a comparative analysis of our findings in relation to the previous researcher. In order to carry out these extensive simulations, we utilised the finite element method, explicitly employing the ANSYS/Explicit Dynamic solver AUTODYN and implementing a simplified 2D Axisymmetric model. A series of ballistic experiments were conducted using various combinations of Alumina and Weldox 460 E steel panels, covering a wide range of bullet velocities. Our analysis focused on seven-panel combinations, namely WL12, AL5+WL5, AL5+WL10, AL10+WL5, AL10+WL10, AL12+WL12, and AL15+WL15, each of which was distinct from the others. The results obtained from our calculations indicate that both the AL12+WL12 and AL15+WL15 panel configurations have met the stringent requirements of the National Institute of Justice (NIJ) Type IV standard in terms of their ability to withstand projectiles. The AL12+WL12 configuration demonstrated a depth of penetration (DOP) of 23 mm, a deflection of 4.3 mm, and a Velocity Ballistic Limit (Vbl) of 954.68m/s. The AL15+WL15 arrangement demonstrated notable performance, with a DOP of 21 mm, a deflection of 1.4 mm, and an impressive Vbl of 1345.9m/s, which stands in stark contrast to other configurations. The results of our investigation highlight the exceptional performance of the AL15+WL15 panel configuration in resisting NIJ Type IV bullets, thus solidifying its position as the most optimal selection.

1. INTRODUCTION

The issue of ensuring optimal body protection has been a matter of great importance throughout the course of human history. This concern dates back to prehistoric times, when individuals relied on animal skins and raw natural materials for their protective needs. In contemporary military contexts, advanced armor technologies are applied to provide enhanced levels of protection. The advancement of warfare and the enhanced efficiency of rifles and high-velocity ammunition have heightened the urgency for the development of sophisticated protective equipment [1].

The advancement of body protection had a notable progression in 1945 with the introduction of ceramic armor by American Lt Commander Andrew Webster. This innovation played a pivotal role in the development of contemporary military armor technology. Nevertheless, the progression of military armaments into the 21st century has presented a quandary in terms of balancing the need for protection with the requirement for agility. In order to tackle this issue, scholars have directed their attention towards the advancement of durable and lightweight ceramic materials for the purpose of bodily protection [1, 2].

Alumina, SiC, and Boron are prominent ceramic materials commonly employed in numerous applications. Alumina presents itself as a feasible option for bulletproof vests due to its lightweight nature and cost-effectiveness, rendering it particularly suitable for civilian applications. The attainment of the appropriate level of protection, specifically against NIJ 4 type projectiles, can be accomplished by utilizing pure alumina or high-purity alumina materials, such as Coors AD85. Coors AD85 is frequently employed for countering NIJ 3 type

projectiles [1, 2].

In addition to ceramics, iron-based materials, including Weldox steel, have also received considerable interest in the context of body armor applications. Weldox 460 E, which falls under the category of TM steel, exhibits a favorable amalgamation of elevated strength, ductility, and commendable weldability. This is accomplished by means of a meticulously regulated procedure involving rolling and heat treatment [3].

The latest studies in the field of body armor have focused on the utilization of bi-layer armor systems, which involve the integration of a rigid ceramic front surface and an iron-based backing plate. The proposed methodology presents a more lightweight design in contrast to the utilization of single-layer iron armor. The primary function of the ceramic layer is to slow down and diminish the velocity of the projectile, while the accompanying backing plate is responsible for absorbing any remaining energy and preventing the fractured ceramic from dislodging [4-6].

A substantial number of scholars have fervently supported and constructed numerical models that depend on computational techniques, including finite difference and finite element methods [7, 8]. These models are commonly utilized in the field through popular commercial software tools, including ANSYS, ABAQUS, LS-DYNA, and DYNA3D [9-11]. Commercial software packages are occasionally utilized to create simulations that portray the ballistic impact properties of different materials [12-14]. The aforementioned strategies widely acknowledged for its cost and time efficiency in comparison to experimental methods, as it necessitates a reduced number of experiments. Nevertheless, the simulation method requires substantial processing capacity and resources. In general, when simulating material textures, three primary numerical approaches are frequently used to simulate the structural properties of substances: the mesoscale unit-cell-based model [15-19], the full 3D continuum model [20-23], and the pin-joined model [24-27]. In the realm of texture modeling, the pin-jointed and 3D continuum models both take into account the weaving patterns found in fabrics, which involve the integration of warp and weft threads. On the other hand, the unit-cell model simulates woven textures by mixing crossovers [28]. It is imperative to acknowledge that there are instances where achieving a comprehensive understanding and depiction of ballistic effects just by the utilization of experimental, numerical, or analytical approaches can prove to be exceptionally arduous. Consequently, a number of scholars have utilized a blend of experimental, numerical, experiential, and analytical methodologies in order to attain a more holistic understanding and evaluation of significant facts inside the realm of ballistic impact systems [29-34].

A notable investigation was conducted, employing experimental and simulation studies using LS-DYNA software, to scrutinize armor systems featuring bi-layer, mosaic, and honeycomb configurations. The experimental configuration involved the utilization of Aluminum 6061-T6 as the backing plate and Alumina as the front plate. During the experimental experiments, projectiles made of Steel 4340 were utilized at various velocities. The results highlighted the effectiveness of the bi-layer approach in preventing the penetration of a bullet with a velocity of 600m/s, while also avoiding excessive depth [5].

The objective of this paper is to present a thorough examination of the progress made in the development of lightweight body protection materials, with particular emphasis on the utilization of alumina and Weldox 460 E steel in the construction of bulletproof vests. Through a comprehensive analysis of the capabilities and limitations inherent in these materials, our objective is to provide a valuable contribution to the continuous enhancement of body armor. This endeavor aims to guarantee the highest level of safety and protection for both military personnel and civilians. In addition to employing the bi-layer technique for preemptively detecting material fractures in the armor, it is imperative to choose a more robust material capable of withstanding projectile impacts, such as Weldox, for instance. The research undertaken by Dey et al. [3] involved a comparative analysis of iron-based materials, specifically Weldox 900 E, Weldox 700 E, and Weldox 460 E. This analysis was carried out by a combination of experimental experiments and simulations utilizing the LS-DYNA program.

The present study aims to examine the ballistic performance of diverse materials and configurations over a range of impact circumstances. The experimental test panel utilized in the study has a thickness of 12 mm and a diameter of 500 mm. The study utilized three various bullet shapes, namely blunt, conical, and ogival, which were propelled at velocities ranging from 150 m/s to 350 m/s. Significantly, the test findings demonstrate a distinct association between the graph depicting initial velocity and the residual velocity derived from both experimental and simulated data, hence demonstrating consistent patterns. The nose shape of the projectile exerts a significant influence on the ballistic limit velocity of the panel. Conical and ogival projectiles often demonstrate ballistic limit velocities of approximately 300m/s, whereas blunt projectiles tend to exhibit ballistic velocity below 200 m/s. The visual representation of the outcomes pertaining to the three distinct bullet types effectively emphasizes the presence of cracked and punctured panels [3].

The assessment of the ballistic impact efficacy of a two-layer armor system, including a ceramic front surface and a metal support layer, was carried out utilizing a semi-analytical methodology [4]. The simulations were performed using AUTODYN software in a 2D axisymmetric configuration. The results of the simulations indicate that when alumina is used as the front plate and aluminum is used as the backing plate, a ballistic limit velocity (BLV) of around 545m/s to 550m/s is achieved. The numerical simulations consistently yielded set values for the residual velocity of the projectile and the ballistic limit velocity (BLV) of the armor when a 20 mm armor-piercing discarding sabot (APDS) bullet made of tungsten alloy, with precise dimensions, was employed. These simulations were conducted on an alumina/aluminum armor with a geometric ratio matching that of the bullet.

The research employed ABAQUS 3D finite element simulations to investigate the impact of different nose projectile geometries on ductile targets, both single and layered [35]. Weldox 460 E steel plates were employed for the simulations conducted at different inclinations. The steel plates had thicknesses of 12 mm for the single layer configuration and 2×6 mm for the layered combination configuration. Additionally, 1100-H12 aluminum targets were utilised, with thicknesses of 1 mm for the single layer configuration and 2×0.5 mm for the layered combination configuration. The findings indicated that monolithic targets exhibited superior performance to layered targets with the same thickness. The ballistic limit of Weldox 460 E steel, with a thickness of 12 mm, exhibited a 10% increase when subjected to an obliquity of 45º. Similarly, the 1100-H12

aluminium target, which had a thickness of 1 mm, demonstrated a 9.3% increase in the ballistic limit when impacted at an obliquity of 30º, compared to a typical impact scenario. Nonetheless, it was seen that both materials have shown comparable levels of endurance when subjected to both normal and oblique impacts. Furthermore, it was found that conical projectiles were able to penetrate through both materials.

The research centered on analysing monolithic and layered panels fabricated using Weldox 460 E Steel as the selected material [36]. The projectile utilized in the study was of a conical configuration, and computational simulations were performed using the Smoothed Particle Hydrodynamics (SPH) method. The investigation focused on assessing the effects of varying panel thicknesses, ranging from 2 mm to 12 mm, with impact velocities spanning from 80m/s to 405.7 m/s. The study's findings indicate a positive correlation between the thickness of the monolithic target panel and its ballistic resistance. The qualitative agreement between the analytical method and SPH simulations for the layered target was close. However, the analytical method quantitatively yielded a lower prediction for the ballistic limit velocity. This discrepancy can be attributed to the analytical method's omission of panel interactions.

The primary objective of this study was to investigate the impact of prestress on the ballistic performance of bi-layer materials. The present study utilized experimental and computational methodologies [5, 37]. To facilitate the objectives of this research, three target plates were employed, each exhibiting different degrees of prestress. The plates under consideration were fabricated utilizing Alumina for the frontal panel, aluminum alloy 2024-T3 for the posterior plate, and AISI 4340 steel for the arm plate. The numerical simulations were performed using LS-DYNA 3D software with the finite element method (FEM). The velocities considered in the simulations ranged from 300 m/s to 600 m/s. The study's findings suggest that the application of prestress substantially impacts the ballistic performance of bi-layer ceramic composite armor. This effect is particularly prominent when larger amounts of prestress are employed. Using an experimental gas cannon configuration, a research study was conducted to analyze the penetrating capacities of three different projectile shapes (blunt, hemispherical, and conical). This study aimed to quantitatively evaluate the bullets' penetrating capability on a 12 mm thick steel plate composed of Weldox 460 E [38]. The shape of the projectile's nose can significantly impact the energy absorption and potential failure of plate structures during penetration. The numerical analysis employed the LS-DYNA explicit finite element approach, using an adaptive meshing strategy to achieve accurate results for conical projectiles. Implementing an adaptive mesh demonstrates that the ballistic limit velocities for blunt, hemispherical, and conical projectiles are 203.8 m/s, 297.8 m/s, and 278.3 m/s, respectively. Upon reaching its maximum velocity upon impact, the projectile experienced plastic deformation, leading to the dissipation of a substantial proportion of its initial kinetic energy.

Thus, based on previous research, this study implemented changes in the panel preparation procedure using ANSYS/Explicit Dynamic software. The materials selected consisted of Alumina as the front plate and Weldox 460 E Steel as the backing plate, with the projectile used being NIJ Type IV, a 7.62 mm projectile, applying typical velocity and weight best on NIJ standard. This study modified the panel and projectile configurations and validated the simulations by comparing the results with those obtained from experimental tests. In addition, the investigation established essential variables, including the penetration depth, the velocity at which the ballistic limit is reached, the deflection rate, and the degree of deformation exhibited by the projectile and panel.

2. METHODELOGY

This simulation employs the non-linear finite element method to replicate ballistic impact testing, explicitly utilizing ANSYS/Dynamic Explicit with AUTODYN for solving. ANSYS/Dynamic Explicit with AUTODYN solution is chosen due to its widespread usage in reputable journals such as the Journal of Impact Engineering, where ls-dyna and ANSYS are commonly employed. The research serves as verification, validated through experimental studies, such as investigations involving Weldox 460 E material as a panel and a blunt projectile made of Arne Tool Steel weighing 197 grams. The Weldox 460 E panel model, featuring a diameter of 500 mm and a thickness of 12 mm, is represented in a 2D axisymmetric configuration. The blunt projectile is modeled with Von Mises plastic-elastic material incorporating isotropic bilinear hardening, excluding fracture failure [3]. Detailed material properties for the projectile are outlined in Table 1.

The impact ballistics analysis will use two types of projectiles. The first projectile is cylindrical and made of Arne Tool Steel material, chosen for verification by previous research [3]. For this study, modifications will be made to the projectile using a 7.62 mm rifle projectile conforming to the National Institute of Justice (NIJ) Standard-0101.06 type IV standard. The projectile comprises two materials: brass for the core and Steel 4340 for the shell. The physical and mechanical property parameters for these materials are provided in the table. The bullet and panel models utilized are cylinders that can be simplified from 3D models to 2D axisymmetric representations. The bullet and panel models may be shown in Figure 1 and Figure 2 with the axis as Barrett's axisymmetric function [2]. The implementation of axisymmetric simplification can potentially decrease the overall volume of bullets and panels, resulting in a reduction in computational load.

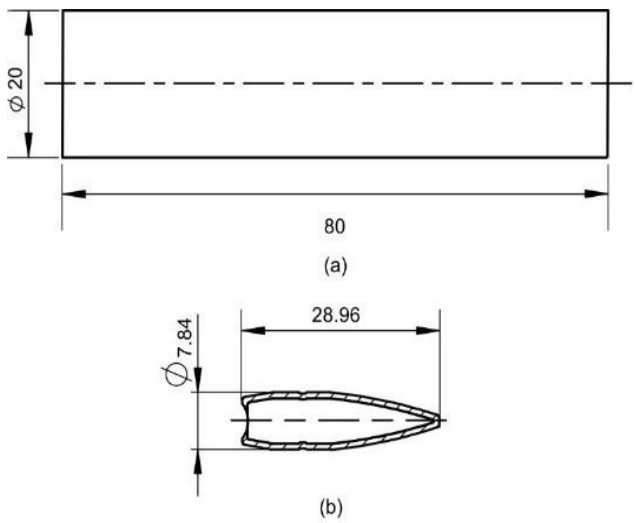

Figure 1. Blunt Projectile and NIJ projectile type IV

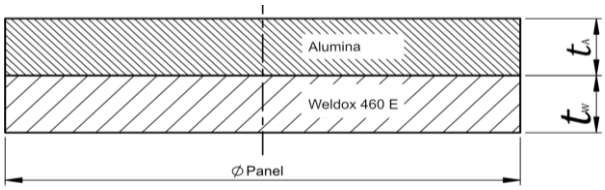

Figure 2. Configuration Panel of Alumina and Weldox 460 E

Table 1. Physical and mechanical of Arne Tool Steel [3]

Parameter	Unit	Value
Density	tonne/m^3	7.85E-09
Young's Modulus	Mpa	2.04E+05
Shear Modulus	Mpa	7.70E+04
Bulk Modulus	Mpa	2.06E+05
Poisson's Ratio		0.33

Table 2. Alumina constants for JH-2 constitutive model [39]

Parameter	Simbol	Unit	Value
Mechanical Properties			
Density	ρ	tonne/m^3	3.89E-09
Johnson-Holmquist Strength Continuous			
Shear Modulus		Mpa	1.52E+05
Hugoniot Elastic Limit Hydrodynamic Tensile Limit	HELT	Mpa	6570
Intact Strength constant	A		0.88
Intact Strength Exponent	N		0.64
Strain Rate Constant	C		0.007
Fracture Strength Constant	B		0.28
Fracture Strength Exponent	m		0.6
Maximum Fracture Strength Ratio	S^f_{max}		1
Damage Constant	D1		0.01
Damage Constant	D2		0.7
Bulking Constant	β		1
Polynomial EOS			
Parameter A1		Mpa	2.31E+05
Parameter A2		Mpa	-1.60E+05
Parameter A3		Mpa	2.77E+06
Parameter B0			0
Parameter B1			0
Parameter T1		Mpa	2.31E+05

Table 3. Physical and mechanical properties of Weldox 460 E, Brass, and Steel 4340 [5, 40, 41]

Parameter	Unit	Value		
		Weldox 460 E	Brass	Steel 4340
		[5]	[40]	[41]
Mechanical Properties				
Density	tonne/m^3	7.85E-09	8.59E-09	7.80E-09
Specific Heat	J/Kg. ℃	452	0.38	477
Poisson's Ratio		0.33	0.34	0.3
Young's Modulus	Mpa	2.10E+05	97000	2.10E+05
Shear Modulus	Mpa	7.89E+04	36194	8.08E+04
Bulk Modulus	Mpa	2.06E+05	1.01E+05	1.75E+05
Johnson Cook Strength				
Initial Yield Stress	Mpa	499	90	792
Hardening Constant	Mpa	382	292	510
Hardening Exponent		0.458	0.31	0.26
Strain Rate Constant		0.0079	0.025	0.014
Thermal Softening Exponent		0.893	1.09	1.03
Melting Temperature	℃	1526.9	1356	1793.1
Reference Strain Rate	1/s	0.0005	1	1
Johnson Cook Failure				
Damage Constant D1		0.636	0.54	0.05
Damage Constant D2		1.936	4.89	3.44
Damage Constant D3		-2.969	-3.03	-2.12
Damage Constant D4		-0.014	0.014	0.002
Damage Constant D5		1.104	1.12	0.61
Melting Temperature	℃	1526.9	1356	1793.1
Reference Strain Rate	1/s	1	1	1

For this study's investigation, the front panel material was modified to Alumina, whereas the rear panel was constructed using Weldox 460 E. The specifications for the properties of Alumina can be found in Table 2, whereas the qualities of Weldox 460 E are listed in Table 3.

Ceramics (Alumina) and metals (Weldox 460 E, Steel 4340, and Brass) comprise the materials utilized in this investigation, which were also applied to the projectiles and panel. In order to represent the properties of materials in simulations involving high-impact loads, it is imperative to incorporate strength and fracture failure criteria. The parameters governing metallic materials' strength and failure mechanisms

adhere to the Johnson and Cook model, wherein the constant parameter values are presented in Table 3. The Johnson and Cook model is utilized to characterize the mechanical response of metallic materials subjected to harsh conditions. Specifically, the materials investigated in this study are Weldox 460 E, Steel 4340, and Brass, representing the metallic materials under consideration. In contrast, the ceramic material model employs the Johnson-Holmquist Strength Continuous (JH-2) constitutive equation. Table 2 contains the parameters of the Johnson-Holmquist Strength Continuous model.

Table 4 illustrates the simplified designation method for each panel: Alumina is denoted as A, and Weldox 460 E as W. These seven selected combinations aim to encompass diverse real-world applications. Typically, alloy anti-ballistic plates are 15-25 mm thick and weigh 2.5-3.5 kg. By utilizing various combinations, the study endeavors to emulate the multifaceted scenarios encountered in real-world settings. This approach ensures comprehensive coverage of potential applications, reflecting the varied demands and requirements within industries where such materials find utility and are easy to produce in large quantities. Through this selection process, the study seeks to provide insights applicable to a broad spectrum of practical situations and challenges.

Table 4. Panel configuration code

Code Panel	Thickness (mm)		Total Thickness (mm)
	Alumina	Weldox 460 E	
WL12	-	12	12
AL5+WL5	5	5	10
AL5+WL10	5	10	15
AL10+WL5	10	5	15
AL10+WL10	10	10	20
AL12+WL12	12	12	24
AL15+WL15	15	15	30

The friction coefficient between the panel and the projectile was neglected in accordance with the research conducted by Dey et al. [3], which is applicable to all variations used in their study. Figure 3 shows that the right side of the panel is locked to prevent movement during impact and is set as a fixed support.

Mesh convergence was performed as a critical stage in the investigation led by Barrett et al. [2] to validate the convergence of the numerical legal procedure. The conducted mesh convergence analysis focused on a cylindrical projectile characterized by a length of 15mm and a diameter of 10mm. The projectile was propelled at a velocity of 300m/s. Deformation and ultimate length of the projectile were determined by the mesh convergence study using variations of 0.0625mm, 0.125mm, 0.25mm, and 0.5mm. The research results revealed that the utilization of a mesh size of 0.25mm, coupled with a linear arrangement, led to convergence. This mesh size particularly was determined to offer adequate precision. The present work used the identical modeling approach as the study conducted by Barrett et al. [2], therefore employing a mesh size of 0.25mm.

The element size and number of elements are important factors in minimizing computational time. In the projectile impact area, a fine mesh is utilized, whilst the sections further out from the impact zone are assigned a coarse mesh. The process of dividing the panel model into three distinct sections is depicted in Figures 3 and 4. The initial segment is divided into three sections, each utilizing a different mesh size: 0.25mm for the first portion, 0.5mm for the second section, and 0.75mm for the third piece positioned at the rightmost extremity of the panel.

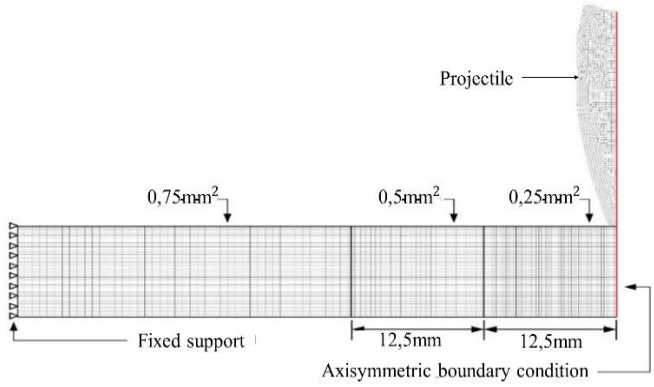

Figure 3. Mesh Modeling and Boundary Condition [2]

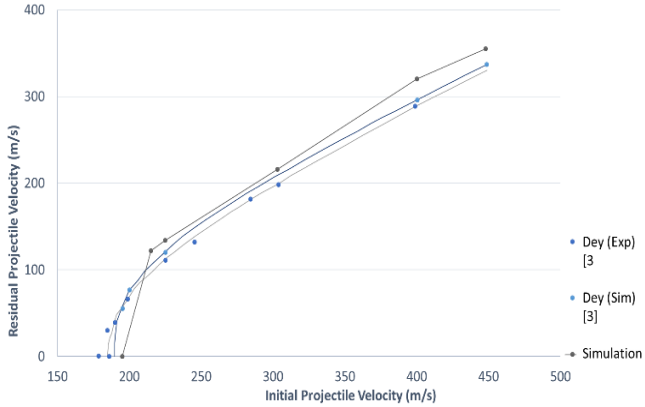

Figure 4. The numerical simulation was utilized to validate the residual velocity [3]

3. RESULT AND DISCUSSION

3.1 Comparison of bullet residual velocity

Conducting a comparative analysis with the experimental findings reported by Dey et al. [3] is crucial for assessing the accuracy of the simulation. In the given context, the projectile being referred to is a blunt bullet constructed from Arnor tool steel. The object possesses a diameter measuring 20 millimeters and exhibits a length of 80 millimeters. The current investigation utilizes a panel constructed from Weldox 460 E steel, which is cylindrical in shape and measures 12 mm in thickness and 500 mm in diameter. The verification method in this specific circumstance entails doing tests at various velocities to evaluate the precision and resilience of the model when subjected to varied loads.

The comparison results between simulations and experiments conducted by Dey et al. [3] are presented in Figure 4 and Table 5. These results specifically focus on the initial velocity profile of flat-nosed (blunt projectile) bullets and the final velocity of bullets in the shoot test. Weldox 460 E Steel panel material was utilized in the execution of the investigations. The residual velocity (Vr) is a commonly used term to represent the velocity of the bullet after it has passed through the thickness of the panel. When the velocity of the bullet, denoted as Vr, is equal to zero meters per second, it signifies that the panel is capable of retaining the bullet. This

residual velocity of zero is referred to as the ballistic limit velocity (Vbl), which serves as a measure of the panel's resistance against ballistic forces.

Table 5. The numerical simulation was utilized to validate the residual velocity [3]

Weldox 460 E Steel Model					
V0 (m/s)	Vr (m/s)			Error (Exp)	Error (Sim)
	Dey (Sim)	Dey (Exp)	Simulation	%	%
215	108.03	100.02	121.92	21.89	12.85
225	120.01	111.03	133.94	20.64	11.61
300	207.35	199.33	216.02	8.37	0.05
400	296.19	298.95	320.20	7.11	8.10
450	337.22	330.41	354.96	7.43	5.26
			Average	13.09	7.58

The examination of the start velocity profile in relation to the residual velocity, as observed in both simulation outcomes, reveals disparities at lower initial bullet velocities. However, it also illustrates a trend of diminishing disparities as the initial bullet velocities increase. The current simulation findings show differences from the study by Dey et al. ranging from 7.58% to 13.09% for initial bullet velocities between 215m/s and 450m/s. The least departure is observed at an initial bullet velocity of 300m/s. These findings are consistent with both the experimental and simulated data presented by Dey et al. [3].

Through an examination of the trendline depicted in Figure 4, it is evident that both curves exhibit a higher degree of precision inside the central region of the curve, namely at a velocity of 300m/s. Hence, the simulation performed in this study aligns with the simulation results reported by Dey et al. pertaining to the bullet velocity of 300m/s. Hence, it is possible to argue that the results obtained from the simulation in this study are consistent with the experimental and simulated results documented by Dey et al. [3].

3.2 Residual velocity profile and depth of penetration

Dey utilized a Weldox 460 E panel material with a dimension of 12mm to fabricate the panel model, which forms the foundation for this study. However, the study done by Dey et al. [3] revealed that the panel's resistance performance did not surpass the specified parameters set forth in the National Institute of Justice (NIJ) Standard-0101.06 type IV standard for projectiles. In order to investigate this topic, the current study makes use of a standard National Institute of Justice 7.62 mm type IV bullet. The results show that a 12-mm-thick Weldox 460 E panel is vulnerable to a bullet traveling at the specified speed. Consequently, a modification is introduced wherein an Alumina front panel is integrated into the Weldox 460 E panel, leading to the creation of a bi-layer panel. The present study aims to examine various panel designs and thicknesses to determine the greatest thickness capable of withstanding the impact of a bullet.

The determination of the ballistic resistance of each design is obtained through the conduct of shooting tests utilizing standard NIJ 7.62 mm type IV rounds, with subsequent measurement of the residual velocities and analysis of their profiles. Figure 5 illustrates the outcomes of the bullet velocity profile in relation to the duration of penetration for various modifications in panel configuration. The penetration time is determined by timing the bullet's motion from the instant it initially encounters the panel until it either passes through or is repelled by the panel. The capacity of the panel to confine the projectile is indicated by a residual velocity of zero. Conversely, if the residual velocity surpasses zero, it signifies that the bullet has successfully passed through the panel. Based on the data presented in Figure 5, it is apparent that the velocity of the projectile experiences a decrease starting at time = 0, which corresponds to the moment when the bullet makes contact with the panel.

This study aims to assess the ballistic resistance of various panel designs by comparing the bullet velocity profiles obtained from simulation shot tests. On the other hand, the research undertaken by Dey et al. [3] using the WL12 panel revealed a residual velocity of 738m/s that was deemed statistically significant. This finding indicates that the panel lacks the capability to withstand the bullet's velocity. The findings of this investigation indicate that the bullet velocity profiles observed on panels AL5+WL5, AL5+WL10, AL10+WL5, and AL10+WL10 continue to display residual velocities, suggesting that these panels are incapable of effectively stopping the bullet. Nevertheless, it has been shown that the augmentation of panel thickness leads to a decrease in residual velocity. The bullet velocity profile for panels with configurations AL12+WL12 and AL15+WL15 declines to zero at approximately 65 μs, indicating that these configurations possess the capability to halt the bullet. Another intriguing observation pertains to the configurations AL5+WL10 and AL10+WL5, wherein the residual velocity on panel AL10+WL5 surpasses that of panel AL5+WL10. This suggests that the Weldox 460 E material exhibits superior effectiveness in bullet resistance when compared to Alumina. Nevertheless, the incorporation of Weldox 460 E material leads to an increased weight, discomfort, and inflexibility of the body armor, owing to the higher mass of Weldox 460 E compared to Alumina.

The incorporation of both materials in a balanced manner will result in a reduced weight, enhanced comfort, and improved flexibility of the body armor when the panel arrangement is applied.

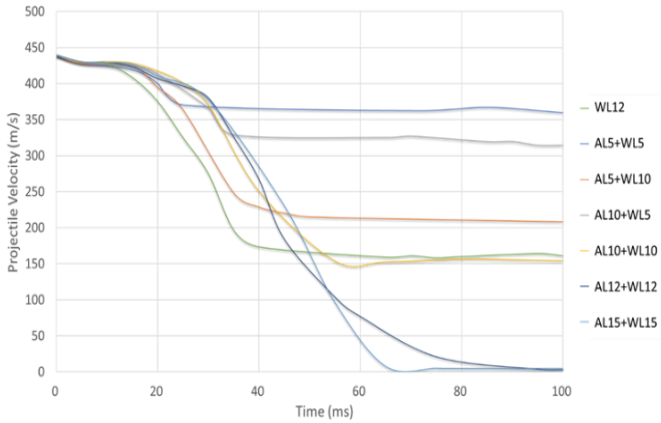

Figure 5. The objective of this study is to analyze the relationship between projectile velocity and penetration time for different panel layouts

Table 6. The ultimate outcome for various panel configurations is ballistic performance

Code Panel	Thickness (mm)		Total (mm)	V0 (m/s)	Vr (m/s)	Vbl (m/s)
	Weldox 460 E	Alumina				
WL12	12	-	12	878	738	782.5
AL5+WL5	5	5	10	878	737	490.625
AL5+WL10	10	5	15	878	419	735.5
AL10+WL5	5	10	15	878	640	510
AL10+WL10	10	10	20	878	314	787.5
AL12+WL12	12	12	24	878	0	954.69
AL15+WL15	15	15	30	878	0	1345.9

Table 7. The end outcomes encompassing mass, drag coefficient of performance (DOP), residual thickness, deflection of thickness, and the ultimate length of the projectile were obtained through the examination of various panel configurations

Code Panel	Mass (kg)	DOP (mm)	tr (mm)	td (mm)	Final Length Projectile (mm)
WL12	18.5	perforated			13.35
AL5+WL5	11.5	perforated			20.83
AL5+WL10	19.2	perforated			15.16
AL10+WL5	15.3	perforated			17.74
AL10+WL10	23.1	perforated			14.81
AL12+WL12	27.7	23.39	4.74	4.3	12.23
AL15+WL15	34.6	21.06	10.25	1.4	11.05

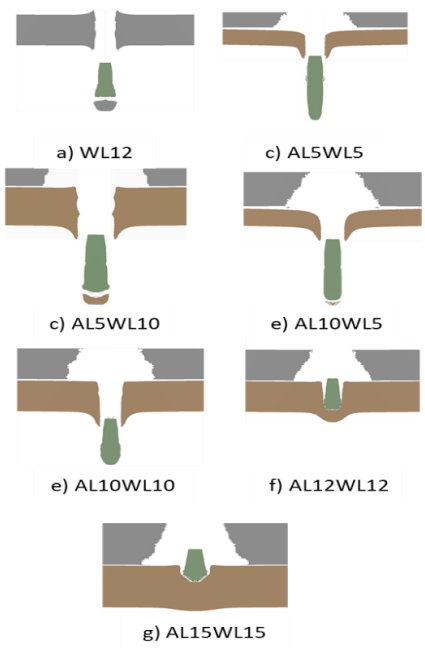

Figure 6. Bullet Penetration visualization with multiple panel configurations

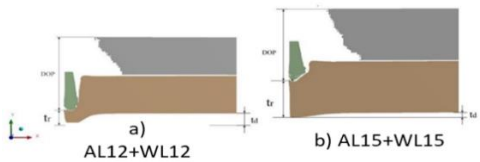

Figure 7. Schematic depth of penetration

Based on the statistical data shown in Tables 6 and 7, it can be deduced that the WL12 panel lacks the capacity to endure the velocity of the NIJ 7.62mm bullet at 878m/s. The AL12+WL12 panel design demonstrates efficacy in halting the projectile's motion by attaining a residual velocity of zero, which is confirmed by the observations. It should be highlighted, nonetheless, that the panel's total thickness of 24 mm results in a 23 mm penetration depth and a 4.3 mm deflection. On the other hand, the panel configuration of AL15+WL15 exhibits a higher level of effectiveness in halting the projectile. In spite of the 30 mm total panel thickness, this setup results in a zero residual velocity, 21mm of penetration, and 1.4mm of deflection. Based on the findings presented in Figures 6 and 7, it is evident that the AL15+WL15 panel configuration demonstrates a higher level of performance in comparison to alternative configurations of layered panels including Alumina and Weldox 460 E materials. The AL15+WL15 configuration demonstrates effective interception capabilities against the NIJ 7.62 mm projectile, which is propelled at a velocity of 878 m/s.

3.3 Residual velocity profile with variation of projectile initial velocity

The residual velocity profiles of bullets with different beginning velocities on multiple panel layouts are depicted in Figure 8. It is necessary to ascertain the ballistic resistance of the panels. Moreover, the observed disparity in residual velocities among various panel configurations exhibits a consistent pattern: an augmentation in the initial bullet velocity leads to elevated residual velocities.

In order to evaluate the ballistic resistance of the panels, it is necessary to estimate the Velocity Ballistic Limits (Vbl) value, which is obtained by measuring the residual velocity when it reaches 0m/s. The velocity value (Vbl) for the WL12 panel, which serves as a reference material, is measured to be 782.5 m/s. Based on the analysis of panel configurations and the WL12 material, it is observed that the AL5+WL5, AL5+WL10, and AL10+WL5 panels exhibit lower Vbl values compared to the WL12 panel. Conversely, the AL10+WL10 panel demonstrates a Vbl value that is nearly indistinguishable from that of the WL12 panel. In contrast, the AL12+WL12 and AL15+WL15 panels exhibit elevated Vbl values in comparison to the WL12 panel. Therefore, panels possessing higher Vbl values are indicative of superior ballistic protection against bullet velocities. The panel's structural integrity can be

compromised when the initial velocity of a bullet exceeds the ballistic limits, resulting in the penetration of the panel. Therefore, the augmentation of panel designs by the use of Alumina material has the potential to improve the panels' ability to withstand ballistic impacts. Based on the findings of the investigation, it can be concluded that the AL5+WL5 panel has the lowest Vbl value at 490.625 m/s, whereas the AL15+WL15 panel exhibits the highest Vbl value at 1795 in.

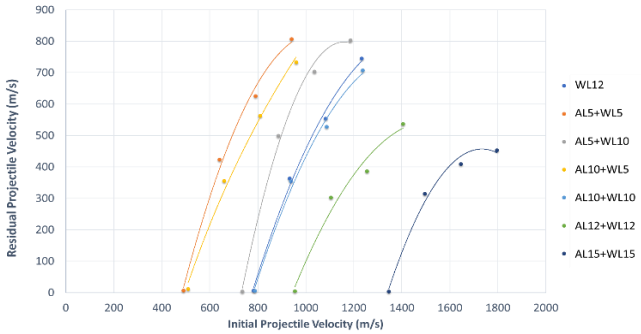

Figure 8. Bullet Residual Velocity Profile against Initial velocity of the bullet in the configuration panel

3.4 Friction variation

The panel and projectile deformation in relation to variations in friction are illustrated in Figure 9. The present study involved the application of frictional changes to panel AL15+WL15. The objective of these fluctuations in friction was to ascertain the coefficient of friction between the panels. According to the data presented in Table 8, the depth of penetration was found to be the lowest when the frictional value was 0, whilst the largest depth of penetration was seen at a frictional value of 0.5.

In the context of the thickness residual, it was seen that the minimum value was recorded at a frictional coefficient of 0.9, measuring 8.29 mm. Conversely, the maximum thickness residual value of 10.25 mm was observed at a frictional coefficient of 0. The deflection value with the lowest thickness was recorded at a frictional coefficient of 0, measuring 1.40 mm, while the highest value of 1.76 mm was observed at a frictional coefficient of 0.9. In regards to the ultimate length of the projectile, the minimum measurement of 11.05 mm was recorded during a frictional condition of 0, while the maximum measurement of 11.39 mm was seen under a frictional condition of 0.9.

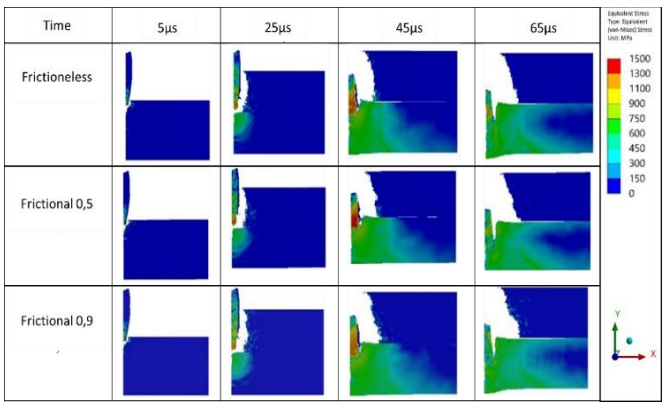

Figure 9. The study focuses on the deformation of projectiles and panels in the presence of differences in friction

Table 8. Frictional Variation

Frictional	DOP (mm)	tr (mm)	td (mm)	Final Length Projectile(mm)
0	21.06	10.25	1.40	11.05
0.5	21.89	8.48	1.67	11.29
0.9	21.86	8.29	1.76	11.39

3.5 Deformation patterns of projectiles and panels

In order to comprehend the ballistic resistance phenomenon resulting from the integration of Alumina panels with Weldox 460 E material, a comprehensive analysis of the design is important. Furthermore, it is essential to scrutinize the deformation patterns exhibited by the panels and bullets during the ballistic simulation. The forthcoming assessment will mostly concentrate on panels WL12, AL12+WL12, and AL15+WL15. Figure 10 depicts the deformation patterns of the bullets in the three panel models (WL12, AL12+WL12, and AL15+WL15) at distinct instances of penetration (s=5µs, 25µs, 45µs, and 65µs).

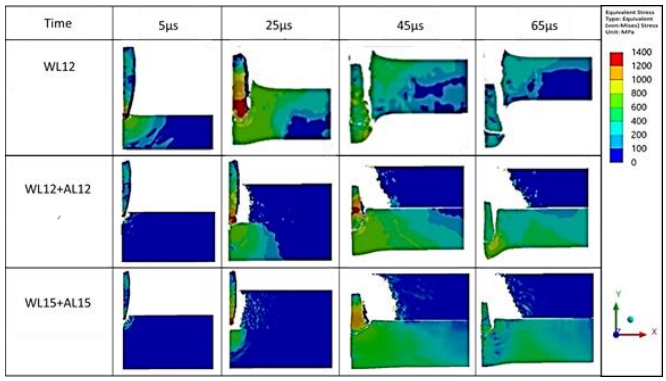

Figure 10. This study investigates the stress propagation characteristics of three panel configurations: WL12, AL12+WL12, and AL15+WL15

The projectile's core begins to pierce the target panel at 5µs, when it reaches the thickness of the panel. Within the WL12 panel, it is observed that the brass outer layer of the projectile's jacket undergoes separation from the inner structure of the bullet. Nevertheless, it is seen that in the AL12+WL12 and AL15+WL15 panels, the jacket layer stays undamaged while the bullet successfully infiltrates the alumina ceramic panel. The panels exhibit apparent disparities in deformation. Specifically, in the WL12 panel, the bullet's penetration just results in the production of a hole, characterized by a size that closely approximates the cross-sectional dimensions of the bullet. The observed deformation in the Weldox 460 E material can be attributed to its inherent ductility and relatively low Young's modulus. The study [3] saw a comparable phenomenon wherein a ductile hole was formed during the process of penetration.

Conversely, projectile penetration in the AL12+WL12 and AL15+WL15 panels produces apertures that are larger in size than the cross-section of the bullet. Upon impact with the target panel, the bullet's core successfully infiltrates the target, but the jacket stays undamaged. This phenomenon arises due to the inherent brittleness and elevated Young's modulus of ceramic materials. The target panels exhibit the presence of fragile perforations resulting from the impact of the projectile. The second layer is the Weldox 460 E layer, which is

penetrated by bullets at 25 μs and 45 μs in the AL12+WL12 and AL15+WL15 panels. The deformation pattern seen in both configurations exhibits a resemblance to that of the WL12 panel, wherein bullet penetration results in the development of ductile holes. At a duration of 65 microseconds, the bullet's ability to enter the AL12+WL12 and AL15+WL15 panels ceases, but in the case of the WL12 panel, the bullet achieves complete penetration.

4. FUTURE HIGHLIGHTS

For the development of bulletproof plates, a significant transition toward a greater reliance on simulation methodologies is anticipated shortly. This methodology offers a cost-effective and time-efficient substitute for conventional experimental techniques [42]. It holds the possibility of enhancing plate designs and achieving a complete comprehension of ballistic impact behavior. The superiority of the AL15+WL15 panel configuration for ballistic applications, particularly in its resistance against NIJ Type IV bullets, is apparent due to its exceptional performance compared to alternative tested configurations.

The rationale for this determination is derived from the comprehensive assessment carried out in the study, which includes ballistic experiments and simulations, as well as the exact comparison of outcomes with established benchmarks and prior investigations. Nevertheless, it is crucial to recognize that the precise determination may differ based on the distinct objectives and demands of the specific application or industry utilizing these components. The ultimate decision may also be influenced by factors such as cost considerations and environmental conditions [43-45].

To summarize, the crucial role of simulation approaches will considerably affect the future landscape of bulletproof plate design. Computational models, implemented using finite element methods (FEMs) and popular commercial software such as ANSYS and LS-DYNA, provide a cost-effective and time-efficient approach to enhancing ballistic performance. The primary emphasis will center on the continual enhancement of numerical simulations using novel methodologies, facilitating the advancement of increasingly efficient bullet-resistant materials.

5. CONCLUSIONS

During the NIJ Type IV Standard Shot Test Simulation, the use of Weldox 460 E steel and alumina panels with varying thicknesses produced significant outcomes. This study undertakes a comparative analysis of bullet residual velocity simulations, contrasting with prior research by Dey et al. Discrepancies between the two sets of results are evident, with experimental data showing an average deviation of 13.09%, while simulations exhibit a more favorable average deviation of 7.58%. These findings underscore the efficacy of utilizing different materials and thicknesses in constructing anti-projectile panels. The observed disparities highlight the importance of comprehensive simulation studies in enhancing understanding and refining protective measures.

There is a range of performance levels among the array of panel configurations designed to comply with the NIJ Type IV standard. The panels labeled WL12, AL5+WL5, AL5+WL10, AL10+WL5, and AL10+WL10 demonstrate insufficiency in withstanding the initial velocity of the bullet, which measures 878 m/s. On the other hand, it can be observed that the AL12+WL12 and AL15+WL15 panels demonstrate a notable ability to endure the impact of projectiles. Out of the many configurations considered, it is seen that the AL15+WL15 panel exhibits the most limited depth of penetration, measuring 21mm. As the thickness of the panel increases, there is a corresponding increase in the Velocity Ballistic Limit (Vbl). For instance, when the panel thickness reaches 30 mm, the Ballistic limit value surpasses 1345.9m/s.

An analysis of the deformation patterns of the projectile and panels demonstrates discernible characteristics. The separation of the brass material jacket from the bullet's core in the WL12 panel can be attributed to the existence of ductile holes or a low Young's modulus. On the other hand, it is seen that the jacket layer in the AL12+WL12 and AL15+WL15 panels remains undamaged when subjected to bullet penetration. This phenomenon can be linked to the presence of brittle holes or a high Young's modulus within the alumina ceramic panel.

The results of this study provide significant contributions to the understanding of the behaviour and performance of anti-projectile panels made of Alumina and Weldox 460 E Steel. We recommend to AL12+WL12 and AL15+WL15 composition to use in real conditions. As a result, these findings advance the field of ballistic protection materials and design. The utilization of these findings in subsequent study and advancements holds the capacity to augment the overall safety and efficacy of body armor and protective equipment in various contexts.

ACKNOWLEDGMENT

The authors thank to Universitas Sebelas Maret under the research scheme of Penelitian Unggulan Terapan 2023.

REFERENCES

[1] Commander, L., Webster, A. (2019). 11-Alumina in lightweight body armor. Alumina Ceramics, 2019: 321-368. https://doi.org/10.1016/B978-0-08-102442-3.00011-7

[2] Barrett, S.A., Christiansen, R., Otham. (2016). Ballistic Properties of Projectile material. Aalborg University, https://projekter.aau.dk/projekter/files/249530927/DMS3_2225a.pdf.

[3] Dey, S.A., Børvik, T., Hopperstad, O.S., Leinum, J.R., Langseth, M. (2004). The effect of target strength on the perforation of steel plates using three different projectile nose shapes. International Journal of Impact Engineering, 30(8-9): 1005-1038. https://doi.org/10.1016/j.ijimpeng.2004.06.004

[4] Chi, R., Serjouei, A., Sridhar, I., Tan, G.E. (2013). Ballistic impact on bi-layer alumina/aluminium armor: A semi-analytical approach. International Journal of Impact Engineering, 52: 37-46. https://doi.org/10.1016/j.ijimpeng.2012.10.001

[5] Zhao, Z.N., Han, B., Li, F.H., Zhang, R., Su, P.B., Yang, M., Zhang, Q., Zhang, Q.C., Lu, T.J. (2020). Enhanced bi-layer mosaic armor: experiments and simulation. Ceramics International, 46(15): 23854-23866. https://doi.org/10.1016/j.ceramint.2020.06.162

[6] Flores-Johnson, E.A., Saleh, M., Edwards, L. (2011). Ballistic performance of multi-layered metallic plates impacted by a 7.62-mm APM2 projectile. International Journal of Impact Engineering, 38(12): 1022-1032. https://doi.org 10.1016/j.ijimpeng.2011.08.005
[7] Umbricht, G.F., Tarzia, D.A., Rubio, A.D. (2022). Determination of two homogeneous materials in a bar with solid-solid interface. Mathematical Modelling of Engineering Problems, 9(3): 568-576. https://doi.org/10.18280/mmep.090302
[8] Abdair, D.A., Abbas, A.M., Hussain, H.K. (2022). Punching shear behavior of flat slab strengthen with y-type perfobond shear. Mathematical Modelling of Engineering Problems, 9(4): 1095-1106. https://doi.org/10.18280/mmep.090428
[9] Azzawi, M.M., Hadi, A.S., Abdullah, A.R. (2023). Finite element analysis of crankshaft stress and vibration in internal combustion engines using ANSYS. Mathematical Modelling of Engineering Problems, 10(3): 1011-1016. https://doi.org/10.18280/mmep.100335
[10] Attari, S., Rebhi, R., El-Hadj, A.A., Ikumapayi, O.M., Al-Dujaili, A.Q., Abdulkareem, A.I., Humaidi, A.J., Lorenzini, G., Menni, Y. (2023). Thermo-Mechanical modeling and simulation of impact and solidification of an aluminum particle. Mathematical Modelling of Engineering Problems, 10(2): 389-397. https://doi.org/10.18280/mmep.100201
[11] Boushi, A., Naimi, S. (2023). Optimization of hollow core slab strength based on SFRC orientation. Mathematical Modelling of Engineering Problems, 10(1): 109-118. https://doi.org/10.18280/mmep.100112
[12] Kumar, S., Gupta, D.S., Singh, I., Sharma, A. (2010). Behavior of kevlar/epoxy composite plates under ballistic impact. Journal of Reinforced Plastics and Composites, 29(13): 2048-2064. https://doi.org/10.1177/0731684409343727
[13] D'Amato, E. (2001). Finite element modeling of textile composites. Composite Structures, 54(4): 467-475. https://doi.org/10.1016/S0263-8223(01)00119-2
[14] Lim, C.T., Shim, V.P.W., Ng, Y.H. (2003). Finite-element modeling of the ballistic impact of fabric armor. International Journal of Impact Engineering, 28(1): 13-31. https://doi.org/10.1016/S0734-743X(02)00031-3
[15] Kawabata, S., Niwa, M., Kawai, H. (1973). 4-The finite-deformation theory of plain-weave fabrics. Part II: The uniaxial-deformation theory. The Journal of The Textile Institute, 64(2): 47-61. https://doi.org/10.1080/00405007308630417
[16] Kawabata, S., Niwa, M., Kawai, H. (1973). 5-The finite-deformations theory of plain-weave fabrics. Part III: The shear-deformation theory. The Journal of The Textile Institute, 64(2): 62-85. https://doi.org/10.1080/00405007308630418
[17] Grujicic, M., Bell, W.C., Arakere, G., He, T., Cheeseman, B.A. (2009). A meso-scale unit-cell based material model for the single-ply flexible-fabric armor. Materials & Design, 30(9): 3690-3704. https://doi.org/10.1016/j.matdes.2009.02.008
[18] King, M.J., Jearanaisilawong, P., Socrate, S. (2005). A continuum constitutive model for the mechanical behavior of woven fabrics. International Journal of Solids and Structures, 42(13): 3867-3896. https://doi.org/10.1016/j.ijsolstr.2004.10.030
[19] Nadler, B., Papadopoulos, P., Steigmann, D.J. (2006). Multiscale constitutive modeling and numerical simulation of fabric material. International Journal of Solids and Structures, 43(2): 206-221. https://doi.org/10.1016/j.ijsolstr.2005.05.020
[20] Talebi, H., Wong, S.V., Hamouda, A.M.S. (2009). Finite element evaluation of projectile nose angle effects in ballistic perforation of high strength fabric. Composite Structures, 87(4): 314-320. https://doi.org/10.1016/j.compstruct.2008.02.009
[21] Nilakantan, G., Keefe, M., Wetzel, E.D., Bogetti, T.A., Gillespie Jr, J.W. (2011). Computational modeling of the probabilistic impact response of flexible fabrics. Composite Structures, 93(12): 3163-3174. https://doi.org/10.1016/j.compstruct.2011.06.013
[22] Nilakantan, G., Keefe, M., Wetzel, E.D., Bogetti, T.A., Gillespie Jr, J.W. (2012). Effect of statistical yarn tensile strength on the probabilistic impact response of woven fabrics. Composites Science and Technology, 72(2): 320-329. https://doi.org/10.1016/j.compscitech.2011.11.021
[23] Nilakantan, G., Wetzel, E.D., Bogetti, T.A., Gillespie Jr, J.W. (2012). Finite element analysis of projectile size and shape effects on the probabilistic penetration response of high strength fabrics. Composite Structures, 94(5): 1846-1854. https://doi.org/10.1016/j.compstruct.2011.12.028
[24] Novotny, W.R., Cepuš, E., Shahkarami, A., Vaziri, R., Poursartip, A. (2007). Numerical investigation of the ballistic efficiency of multi-ply fabric armours during the early stages of impact. International Journal of Impact Engineering, 34(1): 71-88. https://doi.org/10.1016/j.ijimpeng.2006.07.001
[25] Zeng, X.S., Shim, V.P.W., Tan, V.B.C. (2005). Influence of boundary conditions on the ballistic performance of high-strength fabric targets. International Journal of Impact Engineering, 32(1-4): 631-642. https://doi.org/10.1016/j.ijimpeng.2005.06.011
[26] Laible, R. (2012). Ballistic Materials and Penetration Mechanics. Elsevier, Amsterdam - Oxford - New York.
[27] Termonia, Y. (2004). Impact resistance of woven fabrics. Textile Research Journal, 74(8): 723-729. https://doi.org/10.1177/004051750407400811
[28] Chu, Y. (2015). Surface modification to aramid and UHMWPE fabrics to increase inter-yarn friction for improved ballistic performance. The University of Manchester (United Kingdom).
[29] Shaktivesh, Nair, N.S., Naik, N.K. (2015). Ballistic impact behavior of 2D plain weave fabric targets with multiple layers: Analytical formulation. International Journal of Damage Mechanics, 24(1): 116-150. https://doi.org/10.1177/1056789514524074
[30] Mohamadipoor, R., Zamani, E., Pol, M.H. (2018). Analytical and experimental investigation of ballistic impact on thin laminated composite plate. International Journal of Applied Mechanics, 10(2): 1850020. https://doi.org/10.1142/S1758825118500205
[31] Sikarwar, R.S., Velmurugan, R., Madhu, V. (2012). Experimental and analytical study of high velocity impact on Kevlar/Epoxy composite plates. Central European Journal of Engineering, 2: 638-649. https://doi.org/10.2478/s13531-012-0029-x
[32] Chen, X., Zhou, Y., Wells, G. (2014). Numerical and experimental investigations into ballistic performance of hybrid fabric panels. Composites Part B: Engineering, 58: 35-42.

https://doi.org/10.1016/j.compositesb.2013.10.019
[33] Soydan, A.M., Tunaboylu, B., Elsabagh, A.G., Sarı, A.K., Akdeniz, R. (2018). Simulation and experimental tests of ballistic impact on composite laminate armor. Advances in Materials Science and Engineering, 2018: 1-12. https://doi.org/10.1155/2018/4696143
[34] Chandekar, G.S., Kelkar, A.D. (2014). Experimental and numerical investigations of textile hybrid composites subjected to low velocity impact loadings. The Scientific World Journal, 2014. https://doi.org/10.1155/2014/325783
[35] Iqbal, M.A., Gupta, G., Gupta, N.K. (2010). 3D numerical simulations of ductile targets subjected to oblique impact by sharp nosed projectiles. International Journal of Solids and Structures, 47(2): 224-237. https://doi.org/10.1016/j.ijsolstr.2009.09.032
[36] Xiao, Y., Dong, H., Zhou, J., Wang, J. (2017). Studying normal perforation of monolithic and layered steel targets by conical projectiles with SPH simulation and analytical method. Engineering Analysis with Boundary Elements, 75: 12-20. https://doi.org/10.1016/j.enganabound.2016.11.004
[37] Zhang, R., Han, B., Li, L., Zhao, Z.N., Zhang, Q., Zhang, Q.C., Ni, C.Y., Lu, T.J. (2019). Influence of prestress on ballistic performance of bi-layer ceramic composite armors: Experiments and simulations. Composite Structures, 227: 111258. https://doi.org/10.1016/j.compstruct.2019.111258
[38] Børvik, T., Dey, S., Clausen, A.H. (2009). Perforation resistance of five different high-strength steel plates subjected to small-arms projectiles. International Journal of Impact Engineering, 36(7): 948-964. https://doi.org/10.1016/j.ijimpeng.2008.12.003
[39] Grujicic, M., Pandurangan, B., d'Entremont, B. (2012). The role of adhesive in the ballistic/structural performance of ceramic/polymer-matrix composite hybrid armor. Materials & Design, 41: 380-393. https://doi.org/10.1016/j.matdes.2012.05.023
[40] Park, C.H., Jo, J.D. (2017). Effect of high hardness armor plate sequences on ballistic impact response. Journal of the Korean Society for Precision Engineering, 34(6): 417-424. https://doi.org/10.7736/KSPE.2017.34.6.417
[41] Johnson, G.R., Cook, W.H. (1985). Fracture characteristics of three metals subjected to various strains, strain rates, temperatures and pressures. Engineering Fracture Mechanics, 21(1): 31-48. https://doi.org/10.1016/0013-7944(85)90052-9
[42] Zhang, L.M., Chao, W.W., Liu, Z. Y., Cong, Y., Wang, Z.Q. (2022). Crack propagation characteristics during progressive failure of circular tunnels and the early warning thereof based on multi-sensor data fusion. Geomechanics and Geophysics for Geo-Energy and Geo-Resources, 8: 172. https://doi.org/10.1007/s40948-022-00482-3
[43] Wang, M., Jin, G., Fu, Y., Liang, J., He, W., Nan, F., Chen, F. (2023). Combustion customization strategy of mixed propellant charges for multi-material additive manufacturing: Simulation and experiment. Arabian Journal of Chemistry, 16(11): 105269. https://doi.org/10.1016/j.arabjc.2023.105269
[44] Wu, S., Xu, Z., Hu, C., Zou, X., He, X. (2022). Numerical simulation study of ballistic performance of Al2O3/aramid-carbon hybrid FRP laminate composite structures subject to impact loading. Ceramics International, 48(5): 6423–6435. https://doi.org/10.1016/j.ceramint.2021.11.186
[45] Alkhatib, F., Mahdi, E., Dean, A. (2021). Design and evaluation of hybrid composite plates for ballistic protection: Experimental and numerical investigations. Polymers, 13(9): 1450. https://doi.org/10.3390/polym13091450